

# Temporal Force Synergies in Human Grasping

Julia Starke, Marco Keller and Tamim Asfour

**Abstract**—Humans can intuitively grasp objects of different shape and weight. Throughout the grasp execution they control and coordinate the grasp forces at all contact points between the hand and the object to achieve a stable grasp. Dexterous grasping with humanoid hands relies on the perfect coordination between grasp posture and force balance at the contact points in a high dimensional space and remains a challenge. In this paper, we present temporal force synergies describing the change in human grasp forces during the grasp execution in a low-dimensional space based on two new grasp synergy models: 1) static force synergies that are derived by a Principal Component Analysis and represent temporal grasp forces as a sequence of time-independent synergy configurations and 2) dynamic force synergies that are learned by a recurrent neural network and encode the temporal change of grasp forces throughout grasp execution in a latent synergy space clustered by grasp types. We show that both synergy spaces encode human grasp forces with an error of less than 2 % and allow the generation of human-like grasp force patterns. Grasp forces for stable grasps described by the dynamic force synergies achieve a grasp quality comparable to demonstrated human grasps in simulation.

## I. INTRODUCTION AND RELATED WORK

Human hands are extraordinarily skillful in their ability to grasp and manipulate objects. They are able to perform versatile and dexterous grasping tasks on arbitrary objects in a flexible and reactive manner and can seamlessly adapt to object properties and the task’s requirements. Endowing anthropomorphic humanoid and prosthetic hands with such abilities remains a challenging problem. The challenge lies not only in the complexity of mechatronics, but in particular in the lack of knowledge of how to implement intelligent control strategies for hand-object interactions. Promising approaches draw inspiration from human hands to reproduce their versatility in terms of design and control. They either introduce taxonomies [1], [2], [3], [4] to structure the search space for grasp synthesis or represent grasps in terms of postural synergies [5] in a low-dimensional space, the synergy or eigengrasp space [6], [7].

The concept of grasp synergies was first revealed in neuroscience [8], [9]. Strong correlations have been shown between the muscle activations controlling the human hand, the so-called muscle synergies [10]. Santello et al. showed correlations also in the joint angles of hand postures for grasping [5]. These postural synergies represent high-dimensional human grasp postures in a low-dimensional parameter space.

This work has been supported by the German Federal Ministry of Education and Research (BMBF) under the project INOPRO (16SV7665) and the Carl Zeiss Foundation under the project JuBot.

The authors are with the Institute for Anthropomatics and Robotics, Karlsruhe Institute of Technology, Karlsruhe, Germany {julia.starke, asfour}@kit.edu

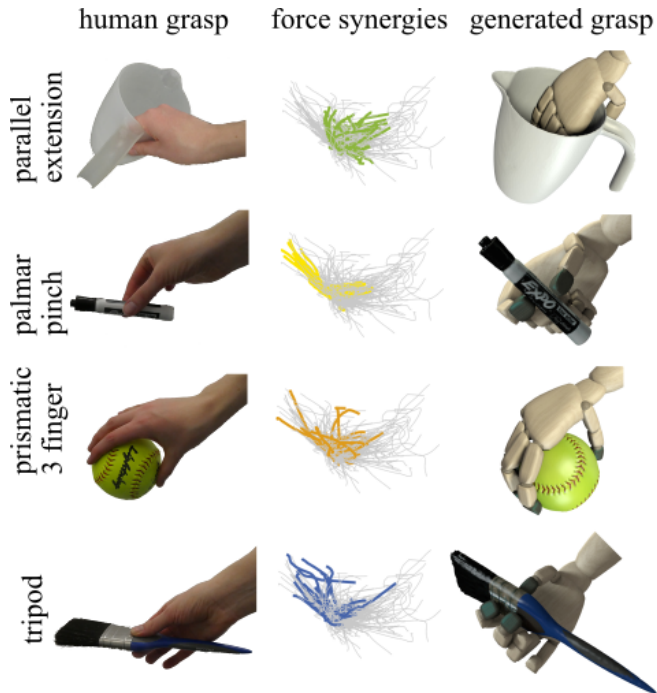


Fig. 1: Representation of grasp contact forces in a low-dimensional synergy space, human grasp force patterns are encoded in a dynamic force synergy space, which allows a separation of different grasp types and the generation of human-like grasp contact forces

For static grasp postures as analyzed by Santello et al., two to three synergy variables are sufficient to represent a wide range of grasp postures. To define the postural synergies, mainly linear dimensionality reduction methods such as *Principal Component Analysis* (PCA) were applied.

Later, postural synergy representations were further analyzed, finding that the number of synergies required to accurately describe a grasp posture significantly depends on the size and variance of the dataset of human grasp postures used for synergy definition [11]. Non-linear methods such as *Gaussian Process Latent Variable Models*, *Kernel PCA* and neural networks were analyzed for synergy definition [12], [13], [14]. Also the concept of grasp synergies was extended to the motion of the fingers from the beginning of the grasp approach phase to the stable grasp posture [15], [16], [17]. A survey on the definition and application of synergies in grasping has been presented in [18].

Such low-dimensional grasp representations provide remarkable insight into the simplification of robot hand design and control. Postural hand synergies have been mechanically implemented for the design of underactuated mechanisms

[19], [20] and entire anthropomorphic robot hands with a small number of motors [21], [22]. The concept of Soft Synergies enables adaptive grasping based on postural synergies [23]. It controls the closing of a robotic hand according to the postural synergies throughout unconstrained motion. But it allows the hand to adapt to the shape of the grasped object, thereby deviating from the rigid postural synergies when the fingers come close to the object surface.

The contact forces applied in a grasp are of equivalent importance for grasp success compared to the hand posture and finger motion. Grasp stability significantly relies on the forces applied at the contact points defined by the grasp [24]. The amount of overall force applied to the object as well as the equilibrium of the forces at the different contact points determine the robustness of the grasp.

The contact points between the hand and the object as well as the forces exerted at these contact points describe the characteristic force configuration of the grasp. However, this force of the stable grasp is only the final configuration of the temporally changing force pattern applied throughout grasp execution. This time-varying distribution of contact forces throughout grasp acquisition will be termed as a temporal force pattern in the following. Once contact with the object is made, the coordination of the forces at the contact locations influence the interaction between the hand and the object.

For robotic hands, grasp forces can be deduced from kinematic postural synergies given compliance models of the hand and the object [25]. However, the compliance of the human hand is challenging to model, especially due to the human's ability to deliberately alter finger stiffness while maintaining the same finger posture. The strategies underlying human grasp force control have been thoroughly analyzed in literature [24], [26].

For opposition power grasps, Santello and Soechting studied tangential and normal forces while grasping a dedicated, sensorized object [27]. They show that the exertion of grasp force is generally performed consistently at the contacts with all five fingers. In particular, they show that correlations in temporal force patterns, force synergies, exist that can be applied for the control of grasp forces. A following study showed that the coordination between forces at the contact locations in the grasp force pattern is determined in the early phases of grasp execution [28]. Based on the existing correlations between grasp contact forces, force configurations of static grasps can be described in an eight-dimensional space of force synergies derived by a PCA [29]. Coordination between the thumb and an opposing virtual finger, that produces forces and moments of all four fingers combined, has been shown based on normal and shear forces in prehensile circular grasps [30].

The contact force patterns characterize opposition primitives of a grasp that are defined by the parts of the hand opposing each other in the grasp posture [31], [32]. Grasp characteristics as the grasp type, object shape and weight influence the force pattern of the grasp [33]. Therefore, these characteristics are related to the control of grasping forces.

In this paper, we present two synergy models for describ-

ing the temporal force patterns that represent the contact forces during the grasp execution. The two models are presented for the low-dimensional representation of human force patterns and the generation of human-like grasp forces as shown in Fig. 1. The first *static synergy model* provides an accurate representation of force patterns in a synergy space independent of time and grasp progress. The second *dynamic synergy model* incorporates the timing information directly into the synergy space to allow the generation of force patterns that are human-like in terms of force distribution and temporal grasp progress. The paper extends the findings of our previous work on static force synergies [29] to the entire temporal force patterns from the first contact with the object until the stable grasp is achieved.

## II. PROBLEM DEFINITION

Our goal is to study temporal change and correlation of normal forces in human grasping and derive a low dimensional representation of grasp force patterns during the different phases of a grasp, i. e. from the initial contact to the final grasp. A grasp  $\mathbf{g}$  is defined by a set of  $n$  contact points  $c_1, c_2, \dots, c_n$  and an  $n$ -dimensional force vector  $\mathbf{f}_g = (f_1, f_2, \dots, f_n)$ , where  $f_i$  is the normal force applied at contact point  $c_i$ . Further,  $\mathbf{f}_g(t)$  with  $t \in [0, T]$  is a time-dependent function that describes the temporal force patterns of a grasp.  $\mathbf{f}_g(t=0)$  is denoting the forces applied at all contact points at the first object-hand contact and  $\mathbf{f}_g(t=T)$  is denoting the forces of the final grasp.

In this work, we use force data from the human handover study recorded at the École Polytechnique Fédérale de Lausanne [29]. This study consists of unscripted human handover and tool use actions on everyday objects of different weights and shapes. The recordings include a variety of different grasping actions. Both the grasping conditions as well as the grasping goal vary within the study. Overall 466 grasps  $\mathbf{g}$  of 16 different grasp types according to the GRASP Taxonomy [4] were recorded on 14 objects. While all recorded grasps are considered to create the synergy space in this work, only seven grasp types are considered to analyze the synergy characteristics of specific grasp types. These grasp types are *power small diameter*, *tripod*, *parallel extension*, *palmar pinch*, *prismatic 3 finger* and *power disk* of which more than 30 recordings are available. In addition *lateral* grasps are considered with 11 demonstrations to represent intermediate and power grasps with the thumb adducted. The combination of grasp types was varied over demonstrations as chosen by the subjects. The contact force between the hand and the object was measured at 18 different locations throughout the hand resulting in a force vector  $\mathbf{f}_g$  of the dimension  $n = 18$ . The grasps are normalized over time and over force to the range of zero to one, corresponding to no contact force and the maximum experimental force respectively.

In our previous work [29], we showed that the contact forces in static stable grasps  $\mathbf{f}_g(T)$  are correlated and can be represented by force synergies  $\mathbf{s}_g$  in an eight-dimensional synergy space  $\mathcal{S}$ . In this paper, we extend the synergy description from static grasp postures to the entire temporal

force patterns  $\mathbf{f}_g(t)$  of a grasp. In other words, we are interested in the identification of temporal synergies  $\mathbf{s}_g(t)$  that encode entire temporal force patterns  $\mathbf{f}_g(t)$  of human grasps including the timing of the grasp progress.

Our approach is twofold. Firstly, we define a static force synergy space to describe grasp force configurations  $\mathbf{f}$  without consideration of the time. Temporal force patterns are then represented as a time-dependent trajectory in this static synergy space. Secondly, we learn dynamic force synergies that directly encode the time of grasp progress. The temporal force pattern is represented directly by a synergy trajectory in the dynamic synergy space. Both synergy models are then evaluated regarding the reproduction and generation of human-like grasp forces.

### III. STATIC FORCE SYNERGY SPACE

We define a synergy space  $\mathcal{S}$  as described in our previous work in [29]. This synergy space is independent of timing and grasp progress and hence encodes static force configurations at a certain time  $t \in [0, T]$ . Each force vector  $\mathbf{f}_{g,t}$  is mapped to a static synergy vector  $\mathbf{s}_{g,t}$ . Temporal trajectories in synergy space are then defined by a series of synergy vectors  $\mathbf{s}_g(t) = (\mathbf{s}_{g,0}, \dots, \mathbf{s}_{g,T})$  according to their chronology. In order to define a generalized description of temporal force synergies for grasps of a specific grasp type, a regression is performed on all temporal sequences of synergies of the same grasp type.

#### A. Static Synergy Description

Proceeding from the static force synergies, a time-agnostic synergy space is defined by a linear PCA taking into account all force configurations  $\mathbf{f}_{g,i}$  for all grasps  $\mathbf{g}$  and all discrete time steps  $i \in [0, T]$  individually. By these means we define a transformation

$$\mathbf{s}_{g,i} = \mathbf{W} \cdot \mathbf{f}_{g,i} \quad (1)$$

that maps forces  $\mathbf{f}$  at time steps  $i$  to the synergy configuration  $\mathbf{s}$ .  $\mathbf{W}$  denotes the weight matrix obtained by the PCA. Similar to the analysis of static grasp forces  $\mathbf{f}_g(T)$  for the stable grasp, eight synergies are needed to represent the original force configurations appropriately. Therefore,  $\mathbf{W}$  is truncated to  $18 \times 8$  dimensions and maps into an eight-dimensional synergy space  $\mathcal{S} \in \mathbb{R}^8$ . Following the method proposed by Romero et al. [12], the temporal sequences of synergies  $\mathbf{s}_g(t)$  can then be described by appending the individual synergy configurations  $\mathbf{s}_{g,i}$  in the chronology of the discrete time steps.

$$\mathbf{s}_g(t) = (\mathbf{s}_{g,i=0}, \dots, \mathbf{s}_{g,i=T}) \quad (2)$$

Trajectories in the synergy space start from the same starting point  $\mathbf{s}_g(0) = \mathbf{s}_{g,0}$ , which characterizes the unobstructed hand having not yet made contact with the object. From there, temporal synergies proceed into different directions depending on the grasp contact points. The first three dimensions of the static synergy space  $\mathcal{S}$  are shown in Fig. 2. Static force synergies  $\mathbf{s}_{g,i}$  are connected to a trajectories  $\mathbf{s}_g(t)$  in synergy space based on the time  $t$  recorded with

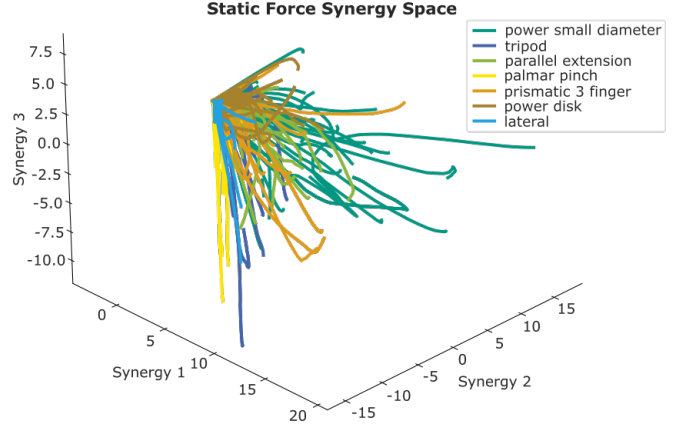


Fig. 2: Force synergy trajectories depicted in the first three dimensions of the static force synergy space  $\mathcal{S}$ , up to 20 recorded synergy trajectories are shown per grasp type

the force pattern  $\mathbf{f}_g(t)$  in human grasping experiments. For the most significant, lower-order principal components, which represent the first synergy dimensions, connections to meaningful grasp characteristics can be drawn by observing the pathway of the individual grasps in synergy space. While the first synergy describes mainly the overall increase of grasp force, the second synergy shows a weighting of forces applied by the index and middle finger. Grasps evolve along a positive direction on the second synergy when a high force is applied at the tip of the middle finger. Respectively, a significant force on the index fingertip, as for example generated by a pinch grasp, results in a negative trend in the second synergy.

#### B. Definition of Generalized Force Patterns

To identify a general trajectory for each grasp type in synergy space, a *Gaussian Mixture Regression* (GMR) is used over all temporal sequences of force synergies associated with the same grasp type. A *Gaussian Mixture Model* (GMM) with five Gaussians is calculated based on the temporal synergies of all grasps with the same grasp type. Gaussians are initialized by k-means clustering and learned with expectation maximization.

The GMR then provides the general expectation  $\mathbf{E}_g(t)$  and the variance  $\mathbf{var}_g(t)$  for each grasp type depending on the time  $t$ . Human-like temporal force patterns for this grasp type can then be generated by defining a synergy sequence  $\mathbf{s}_{new}(t)$  contained within  $\mathbf{var}_g(t)$ . The generalized temporal synergies described by  $\mathbf{E}_g(t)$  are depicted in Fig. 3. Each color represents the generalized sequences of synergies for one grasp type. All eight synergies are plotted along the x-axis and the synergy configurations at each time step are connected by a line. Temporal grasp progress is denoted by the darkness of the line color increasing with time. It can be seen that different grasp types are not entirely separated. However, the generalized synergy trajectories of different grasp types in the static synergy space  $\mathcal{S}$  vary distinguishable.

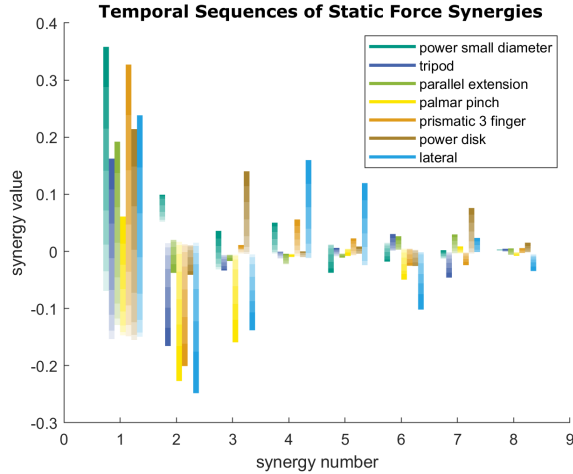


Fig. 3: Synergies generalized for different grasp types in the static synergy space and extended with temporal information by a GMR.

This enables the classification and generation of dedicated, grasp type specific temporal force patterns in this synergy space.

#### IV. DYNAMIC FORCE SYNERGY SPACE

The static synergy space  $\mathcal{S}$  can be used to represent temporal force synergies  $\mathbf{s}_g(t)$  as a chronology of static synergy configurations  $\mathbf{s}_{g,t}$ . However, the synergy representation  $\mathbf{s}_{g,t}$  has no inherent notion of time and grasp progress. This especially means that any information on the variance in grasp execution velocity is lost throughout this synergy description. Notably, the impact of the temporal evolution of grasp forces on the stable grasp force configuration  $\mathbf{f}_g(T)$  cannot be captured by the approach. To overcome this limitation, a deep autoencoder network is trained to represent a dynamic, non-linear force synergy space  $\tilde{\mathcal{S}}$  in latent space.

##### A. Network Architecture and Training

Encoder and decoder are designed as *long-short term memory* (LSTM) networks [34] and trained with entire temporal force patterns  $\mathbf{f}_g(t)$ . By doing this, the information on the time of grasp progress is directly incorporated into the synergy space  $\tilde{\mathcal{S}}$ . Matching the findings of the static synergy representation  $\mathcal{S}$ , the dynamic synergy space is incorporated into a latent layer with eight dimensions, hence  $\tilde{\mathcal{S}} \in \mathbb{R}^8$ . The network is trained with temporal force patterns  $\mathbf{f}_g(t)$  with 46 time steps  $i$ , each describing the force  $\mathbf{f}_g(i) = \mathbf{f}_{g,i}$  with  $i \in [0, T]$ . The network architecture is depicted in Fig. 4.

The encoder consists of two LSTM-layers with 18 and 13 dimensions, respectively. To enforce a continuous synergy representation, the latent space is represented by two dense layers encoding the mean  $\mathbf{E}(\tilde{\mathbf{s}}_g(t))$  and log variance  $\mathbf{var}_{\log}(\tilde{\mathbf{s}}_g(t))$  of the force synergies  $\tilde{\mathbf{s}}_g(t)$  in eight dimensions each. A sample  $\tilde{\mathbf{s}}_g(t)$  from this synergy space is drawn by a downstream sampling layer

$$\tilde{\mathbf{s}}_g(t) = \mathbf{E}(\tilde{\mathbf{s}}_g(t)) + \epsilon \cdot e^{0.5 \mathbf{var}_{\log}(\tilde{\mathbf{s}}_g(t))} \quad (3)$$

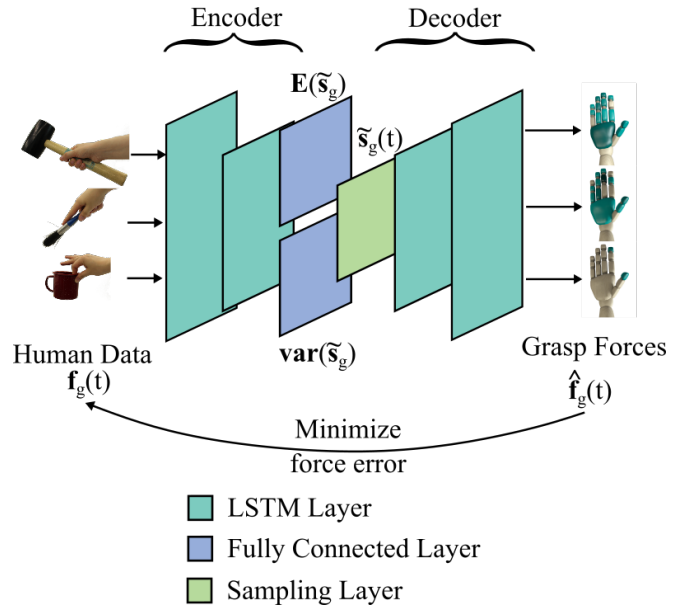


Fig. 4: Structure of the recurrent autoencoder network, mean and variance of the dynamic synergies  $\tilde{\mathbf{s}}_g(t)$  are represented in the latent space trained on the temporal force patterns.

based on the randomly sampled variable  $\epsilon$  with a mean of 0.0 and a standard deviation of 1.0. The synergy sample  $\tilde{\mathbf{s}}_g(t)$  is fed into the decoder network. The decoder is mirroring the encoder architecture back to the 18-dimensional force space. Since contact forces are normalized, a sigmoid activation is applied to all layers short of the last. The output layer has a linear activation function.

Training is performed with a composite loss function  $\mathcal{L}$  explicitly shaping the latent synergy space. A mean squared error term  $\text{MSE}(\mathbf{f}_g(t), \hat{\mathbf{f}}_g(t))$  between the human force pattern  $\mathbf{f}_g(t)$  and the decoder output  $\hat{\mathbf{f}}_g(t)$  is applied. This reconstruction loss ensures an adequate representation of the grasp force patterns by the autoencoder. Following the methodology of our previous work on postural synergies [14], we include an additional loss term to enhance the clustering of grasp types in the synergy space. Due to the temporal structure of the force patterns, a weighted contrastive loss is applied. The distance between sequences of synergies for the grasps  $\mathbf{g}$  and  $\tilde{\mathbf{g}}$  with the same grasp type is minimized to aggregate the synergy representation of similar temporal force patterns. At the same time, separation of dynamic synergies of grasps  $\mathbf{g}$  and  $\mathbf{h}$  from different grasp types is promoted up to a threshold  $d$ . The entire loss function thereby accounts to

$$\begin{aligned} \mathcal{L} = & \alpha \cdot \text{MSE}(\mathbf{f}_g(t), \hat{\mathbf{f}}_g(t)) \\ & + \beta \cdot t \cdot \text{MSE}(\tilde{\mathbf{s}}_g(t), \tilde{\mathbf{s}}_{\tilde{\mathbf{g}}}(t)) \\ & + \gamma(d - t \cdot \text{MSE}(\tilde{\mathbf{s}}_g(t), \tilde{\mathbf{s}}_{\mathbf{h}}(t))) \end{aligned} \quad (4)$$

A description of all symbols is given in Table I. Both latent loss components are multiplied by the normalized grasp execution time  $t$  to gradually emphasize grasp clustering towards the final grasp force configuration  $\mathbf{f}_g(T)$ . This weighting avoids an artificial segregation in the early phase

TABLE I: SUMMARY OF USED SYMBOLS

Symbol	Description
$\mathbf{f}(t)$	human temporal force pattern
$\hat{\mathbf{f}}(t)$	decoded temporal force pattern
$\tilde{\mathbf{s}}(t)$	temporal sequences of synergies
$\text{MSE}(\cdot)$	mean squared error function
$\mathbf{g}, \mathbf{h}$	grasps with different grasp types
$\tilde{\mathbf{g}}$	grasp with the same grasp type as $\mathbf{g}$
$\alpha = 1.0$	weighting parameter
$\beta = 0.05$	weighting parameter
$\gamma = 0.005$	weighting parameter
$d = 0.15$	desired squared distance threshold

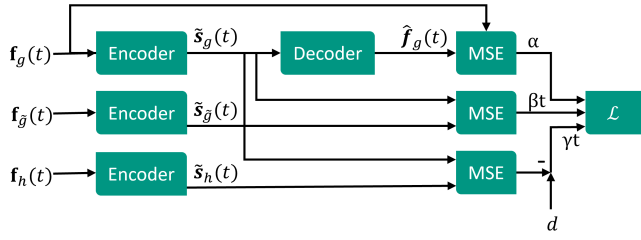


Fig. 5: Loss function to train the autoencoder network, the encoder is evaluated in parallel to allow the comparison of temporal sequences in synergy space

of grasp execution, as force configurations at the first contact are naturally similar over all grasp types. The network is first pretrained for 1500 epochs only based on the reconstruction loss. A similar amount of training is then spent applying the entire loss function  $\mathcal{L}$  to enforce the structured shape of the latent synergy space  $\tilde{\mathcal{S}}$ . An illustration of loss composition is shown in Fig. 5.

The data is split into training, validation and test set at a proportion of 90%, 10% and 10% respectively. For training we use an Adam optimizer with a learning rate of  $10^{-3}$  and gradient norm is scaled to 0.5.

### B. Dynamic Synergy Description

The first three dimensions of the dynamic synergies in the latent space learned by the autoencoder are shown in Fig. 6. The line color of the synergy sequences gets darker over the time of grasp progress. Similar to the static synergies  $\mathbf{s}_g$ , the trajectories  $\tilde{\mathbf{s}}_g(t)$  of human grasp forces in the dynamic synergy space have a common origin marked by a red circle in Fig. 6. From this unconstrained hand configuration without any contact forces, the temporal force patterns evolve into different directions, as can be seen in Fig. 6. The generalized description of different grasp types in the dynamic synergy space calculated by a GMR on all demonstrated dynamic synergies  $\tilde{\mathbf{s}}_g(t)$  of the same grasp type as described in subsection III-B is shown in Fig. 7. It can be seen, that the temporal force patterns of different grasp types are locally separated in synergy space. Especially in the first three synergies, individual grasp types can be clearly distinguished showing a correspondence between the learned synergies and the grasp type. Compared to the static synergy space  $\mathcal{S}$ ,

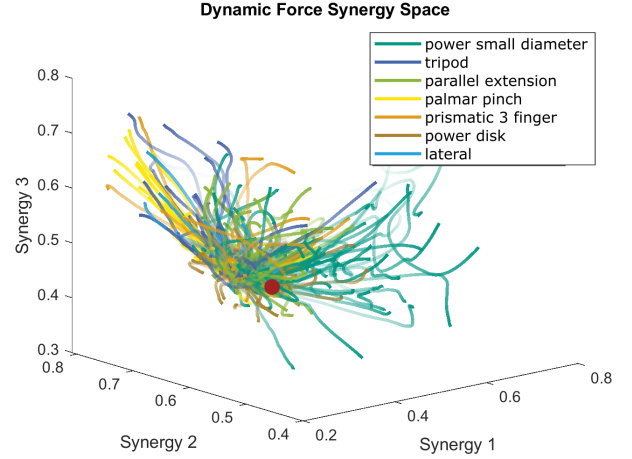


Fig. 6: Force synergy trajectories of different grasp types shown in the first three dimensions of the dynamic synergy space  $\tilde{\mathcal{S}}$ , the red circle marks the center position of  $\mathbf{s}_g(0)$  in synergy space.

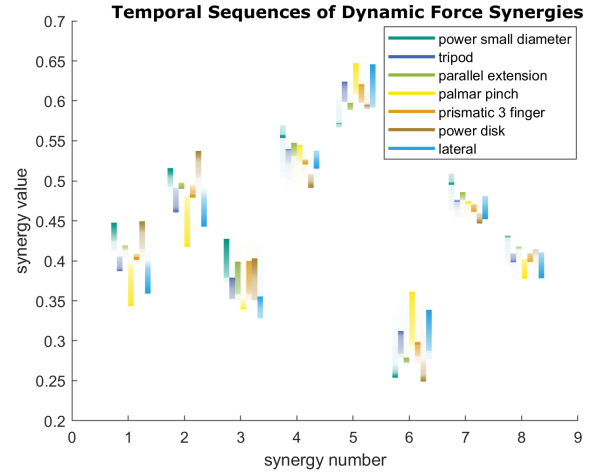


Fig. 7: Synergies generalized for different grasp types by a GMR in the dynamic synergy space.

trajectories in the dynamic synergy space  $\tilde{\mathcal{S}}$  are separated earlier in the grasp progress and do not overlap in any synergy dimension.

## V. EVALUATION

The two force synergy models are evaluated regarding 1) the quality of reproduction and generation of human-like grasp force patterns and 2) the stability of grasps described by dynamic force synergies. As shown in Fig. 2 and Fig. 6, both synergy spaces are shaped differently due to non-linearity and additional grasp clustering of the autoencoder network.

### A. Reproduction Quality

The reproduction error of human grasp forces is defined as the root mean squared error  $\text{RMSE}(\mathbf{f}_g(t), \hat{\mathbf{f}}_g(t))$  between the demonstrated force pattern  $\mathbf{f}_g(t)$  and the force pattern  $\hat{\mathbf{f}}_g(t)$  reconstructed from synergy space. For the static synergy

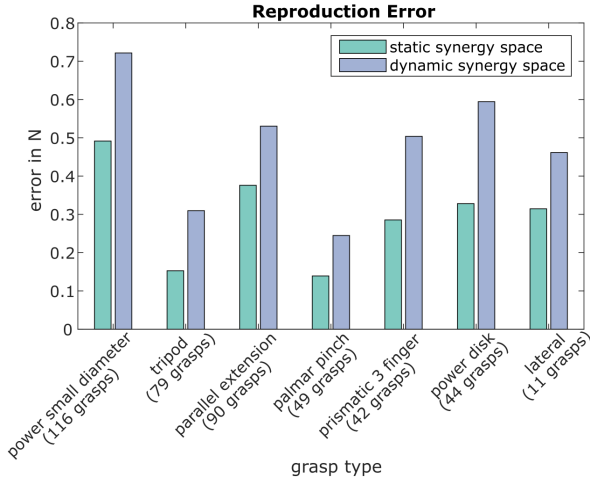


Fig. 8: Mean reproduction error of the force synergies by grasp type calculated over all available recorded data for this grasp type.

space  $\mathcal{S}$ , the mean reproduction error over all recorded grasps is 0.32 N or 0.98 % of the maximum grasp force of 32.4 N. The mean reproduction error for the dynamic synergy space  $\tilde{\mathcal{S}}$  is 0.65 N and 0.61 N for the test set and the entire data set respectively. This corresponds to 1.99 % and 1.88 % of the maximum force.

The mean reproduction error for each grasp type is shown in Fig. 8. It is calculated by averaging over the reproduction error of all grasps recorded for this specific grasp type. The total number of grasps considered for each grasp type is also listed in Fig. 8. Especially precision grasps like *tripod* or *palmar pinch* are represented very well by the synergy models, while the largest error can be observed for *power small diameter*. This is due to a higher variance in the force distribution of power grasps involving many contact points. The grasp type *power small diameter* is very frequently used for both lightweight and heavy objects and the distribution of grasp forces at contact locations varies according to the object’s shape and the task. In contrast, in delicate precision grasps contact points are very well defined and force is distributed over a very small number of contacts. Therefore, the range of valid temporal force patterns for precision grasps is significantly smaller and the exact mapping of these grasps in sequences of synergies is hence simpler.

Overall, the static force synergies thereby show a significantly lower reproduction error, making them the model of choice for the representation of pre-recorded human grasps. However, both models can represent temporal force patterns with an accuracy of more than 98 % and are therefore suitable for grasp force representations in low dimensional spaces.

### B. Generation of Human-Like Grasp Forces

To generate human-like grasp force patterns  $\hat{\mathbf{f}}_g(t)$  based on the synergy model, a sample is taken from the synergy space. For the static force synergy space  $\mathcal{S}$ , a new trajectory in synergy space is sampled within the variance  $\mathbf{var}_g(t)$  of the desired grasp type. The dynamic synergy space  $\tilde{\mathcal{S}}$  directly provides a mean  $\mathbf{E}(\mathbf{s})$  and a variance  $\mathbf{var}(\mathbf{s})$  for

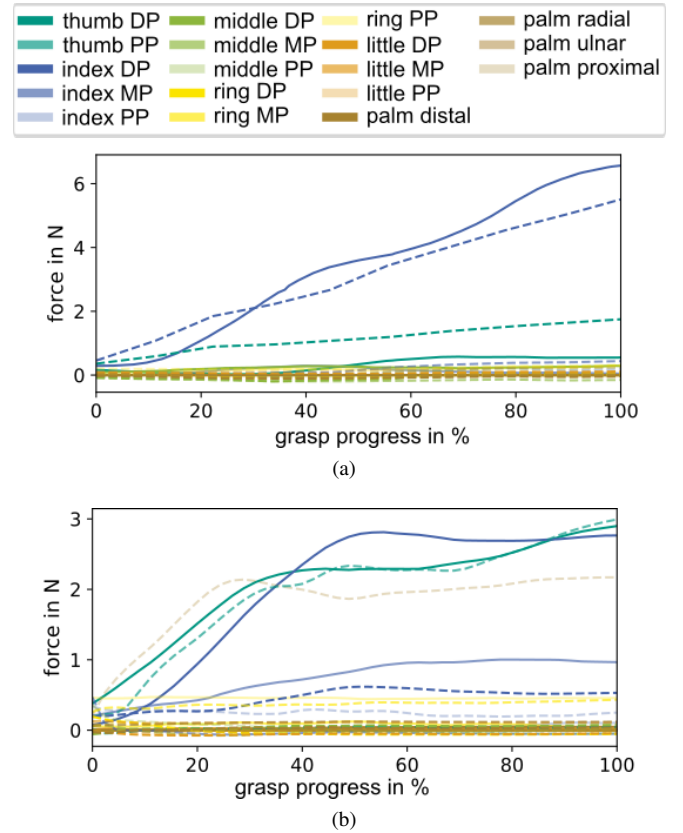


Fig. 9: Temporal force patterns of palmar pinch grasps, force patterns demonstrated by the human are plotted in solid lines while force patterns generated from the static synergy space (a) and dynamic synergy space (b) are shown in dashed lines; forces are described at the proximal (PP), medial (MP) and distal (DP) phalanges of all fingers and within the palm.

every learned temporal force pattern. By taking the pooled mean and variance of all grasps of the same grasp type, the sample range for temporal synergies  $\tilde{\mathbf{s}}_g(t)$  of this grasp type can be defined. Examples of generated temporal force patterns for *palmar pinch* grasps are shown in Fig. 9(a) for the static synergy space  $\mathcal{S}$  and Fig. 9(b) for the dynamic synergy space  $\tilde{\mathcal{S}}$  in dashed lines. Both generated grasps show the desired contact forces along the thumb including the thenar at the proximal palmar location and the index finger. Besides, they differ from the demonstrated human force patterns and thereby allow to adapt the specific force patterns while still keeping human-like force characteristics.

### C. Grasp Quality

The grasp quality of the dynamic force synergies is compared to human grasps in simulation. Since the reproduction quality is lower for the dynamic than for the static synergy space, we aim to verify the feasibility of this force description by a grasp quality evaluation. The grasps are simulated on the human hand model of the Master Motor Map [35]. Simulation and calculation of grasp quality are done using the grasp planning simulator Simox [36]. The evaluation is based on 75 grasps on nine objects used in

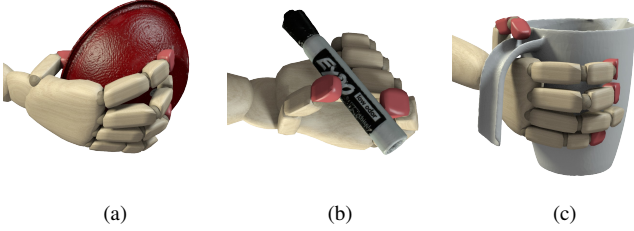


Fig. 10: Simulation of grasps based on force synergies of a parallel extension grasp on a bowl (a), a palmar pinch grasp on a marker (b) and a power small diameter grasp on a pitcher (c).

the human grasp study, of which 3D-models were available. To define the contact points of the hand on the object, we use the human hand position and finger posture from the human grasp recordings. Hand pose and shape are initialized with the recorded human data in simulation. We optimize this initial hand posture according to the contact points measured at the hand and described by the human grasp forces  $\mathbf{f}_g(t = T)$ . Optimization of the hand pose is done by gradually varying the position and orientation of the hand with respect to the object. For each hand pose, the fingers involved in the grasp are closed until contact with the object is made. For grasp stability evaluation, we choose the grasp posture that 1) makes contact with the object at the contact areas measured in the human demonstration and 2) provides the best grasp quality for the demonstrated human grasp forces considering all grasp postures satisfying condition 1). This optimization is necessary to ensure that contact is made at the recorded parts of the hand despite inaccuracies due to measurement error in the hand posture. It is important to note, that both human force configuration and decoded synergy force configuration are evaluated on the same hand posture and hence the same contact points. By these means, a relative comparison between both force configurations independent of the grasp posture is performed. Fig. 10 shows simulations of three grasps on different objects and the parts of the hand that exert a force on the object are marked in red.

Grasp stability is measured by the grasp quality  $\epsilon$ -metric [37], [38]. Overall, the synergy configurations have a very similar grasp quality compared to human force configurations with the mean of  $\epsilon$  being 0.338 and 0.337 respectively. As shown in Fig. 11, the grasp quality varies considerably over grasp types due to the strong dependency of the grasp quality metric on the number of grasp contact points. However, no grasp type shows a significant difference between force synergy configurations and the original demonstrations. This shows that grasp force configurations represented by the dynamic force synergies yield a grasp stability comparable to human grasps.

## VI. CONCLUSION

We introduce two force synergy models to represent the temporal patterns of contact forces throughout the grasp progress. The models describe force synergy patterns by a

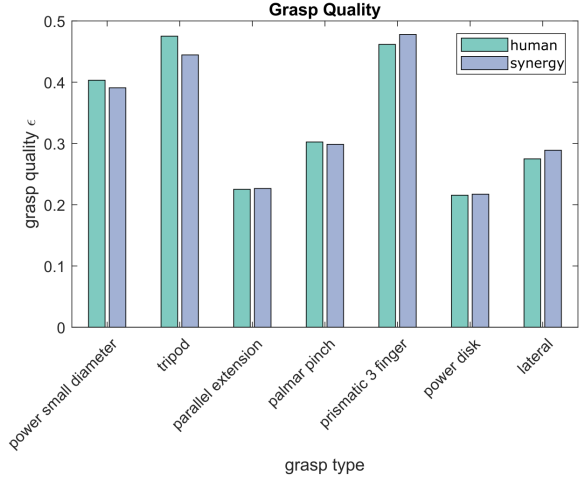


Fig. 11: Grasp quality of simulated grasps with human and synergy forces.

time-dependent trajectory in a linear, static force synergy space  $\mathcal{S}$  and a temporal pattern in a non-linear, dynamic synergy space  $\tilde{\mathcal{S}}$  while taking into account changes of applied forces on the object over time.

The static synergy space provides the best reproduction quality of demonstrated human force patterns. Hence it is well suited for the representation of known human force patterns in a low-dimensional space for the control of robotic hands. However, the static synergy space has no notion of grasp progress and the timing of grasp force patterns generated based on these synergies therefore has to be defined manually.

The dynamic synergy space solves this problem by directly incorporating the timing into the synergy space representation. This ensures that every point in the synergy space is a valid force configuration for the given timestep. The correlation of grasp contact forces throughout the grasp progress is thereby directly learned and grasp force patterns can be generated ensuring a human-like temporal behavior of grasp forces. However, this comes at the cost of a higher error in the reproduction of demonstrated grasps compared to the static synergy space. Nevertheless, the quality of grasps generated from the dynamic force synergies is still comparable to the quality of demonstrated human grasps in simulation. Therefore, the representation accuracy of 98.01% is sufficient for the description of feasible grasp force patterns.

Overall, the static force synergies should be used when a low-dimensional representation of demonstrated force patterns is required. The dynamic force synergies should be preferred, whenever human-like force patterns shall be generated for a known grasp type without a specific human demonstration. Both synergy representations reduce the hand control complexity and could be applied in combination with reinforcement learning strategies for grasping [39].

In future work, we are planning to classify grasps based on the temporal synergies. Further we already started experimenting with neural networks that compress and thereby abstract the time dimension entirely. However, further inves-

tigation is needed regarding temporal smoothing to represent force synergies independent of grasp progress over longer time horizons. In addition, we are planning to apply the dynamic force synergies to control a robotic hand, thereby substantiating the results obtained from simulation on noisy data. We believe that the presented temporal force synergies provide a powerful means to both describe demonstrated grasp force patterns as well as generate force patterns for human-like robot grasps.

## REFERENCES

- [1] J. R. Napier, "The Prehensile Movements of the Human Hand," *The Journal of Bone and Joint Surgery*, vol. 38-B, no. 4, pp. 902–913, 1956.
- [2] M. R. Cutkosky, "On Grasp Choice, Grasp Models, and the Design of Hands for Manufacturing Tasks," *IEEE Transactions on Robotics and Automation*, vol. 5, no. 3, pp. 269–279, 1989.
- [3] N. Kamakura, M. Matsuo, H. Ishii, F. Mitsuboshi, and Y. Miura, "Patterns of Static Prehension in Normal Hands," *The American Journal of Occupational Therapy*, vol. 34, no. 7, pp. 437–445, 1980.
- [4] T. Feix, J. Romero, H.-B. Schmiedmayer, A. M. Dollar, and D. Kragic, "The GRASP Taxonomy of Human Grasp Types," *IEEE Transactions on Human-Machine Systems*, vol. 46, no. 1, pp. 66–77, 2016.
- [5] M. Santello, M. Flanders, and J. F. Soechting, "Postural Hand Synergies for Tool Use," *The Journal of Neuroscience*, vol. 18, no. 23, pp. 10 105–10 115, 1998.
- [6] M. Ciocarlie, C. Goldfeder, and P. Allen, "Dexterous Grasping via Eigengrasps: A Low-dimensional Approach to a High-complexity Problem," in *Robotics: Science & Systems Workshop-Sensing and Adapting to the Real World*, 2007.
- [7] M. T. Ciocarlie and P. K. Allen, "Hand Posture Subspaces for Dexterous Robotic Grasping," *Int. Journal of Robotics Research*, vol. 28, no. 7, pp. 851–867, 2009.
- [8] A. d'Avella, P. Saltiel, and E. Bizzi, "Combinations of muscle synergies in the construction of a natural motor behavior," *nature neuroscience*, vol. 6, no. 3, pp. 300–308, 2003.
- [9] E. J. Weiss and M. Flanders, "Muscular and Postural Synergies of the Human Hand," *Journal of Neurophysiology*, vol. 92, no. 1, pp. 523–535, 2004.
- [10] C. Castellini and P. Van Der Smagt, "Evidence of muscle synergies during human grasping," *Biological Cybernetics*, vol. 107, no. 2, pp. 233–245, 2013.
- [11] N. J. Jarque-Bou, A. Scano, M. Atzori, and H. Müller, "Kinematic synergies of hand grasps: a comprehensive study on a large publicly available dataset," *Journal of NeuroEngineering and Rehabilitation*, vol. 16, no. 63, pp. 1–14, 2020.
- [12] J. Romero, T. Feix, C. H. Ek, H. Kjellström, and D. Kragic, "Extracting Postural Synergies for Robotic Grasping," *IEEE Transactions on Robotics*, vol. 29, no. 6, pp. 1342–1352, 2013.
- [13] P. H. Cui and Y. Visell, "Linear and Nonlinear Subspace Analysis of Hand Movements During Grasping," in *International Conference of the IEEE Engineering in Medicine and Biology Society*, 2014, pp. 2529–2532.
- [14] J. Starke, C. Eichmann, S. Ottenhaus, and T. Asfour, "Human-inspired representation of object-specific grasps for anthropomorphic hands," *International Journal of Humanoid Robotics (IJHR)*, no. 2, p. 2050008, 2019.
- [15] B. A. Kent, J. Lavery, and E. D. Engeberg, "Anthropomorphic Control of a Dexterous Artificial Hand via Task Dependent Temporally Synchronized Synergies," *Journal of Bionic Engineering*, vol. 11, no. 2, pp. 236–248, 2014.
- [16] C. Konnaris, A. A. C. Thomik, and A. A. Faisal, "Sparse Eigenmotions Derived from Daily Life Kinematics Implemented on a Dexterous Robotic Hand," in *IEEE International Conference on Biomedical Robotics and Biomechanics*. IEEE, 2016, pp. 1358–1363.
- [17] H. Marino, M. Gabbicini, A. Leonardis, and A. Bicchi, "Data-Driven Human Grasp Movement Analysis," in *International Symposium on Robotics*, vol. 2016, 2016, pp. 118–125.
- [18] M. Santello, M. Bianchi, M. Gabbicini, E. Ricciardi, G. Salvietti, D. Prattichizzo, M. Ernst, A. Moscatelli, H. Jörmell, A. M. Kappers, K. Kyriakopoulos, A. Albu-Schäffer, C. Castellini, and A. Bicchi, "Hand synergies: Integration of robotics and neuroscience for understanding the control of biological and artificial hands," *Physics of Life Reviews*, vol. 17, pp. 1–23, 2016.
- [19] C. Brown and H. Asada, "Inter-Finger Coordination and Postural Synergies in Robot Hands Via Mechanical Implementation of Principal Components Analysis," in *IEEE/RSJ Int. Conf. on Intelligent Robots and Systems*, 2007, pp. 2877–2882.
- [20] J. B. Rosmarin and H. H. Asada, "Synergistic Design of a Humanoid Hand with Hybrid DC motor-SMA Array Actuators Embedded in the Palm," in *IEEE Int. Conf. on Robotics and Automation*, 2008, pp. 773–778.
- [21] N. Fukaya, S. Toyama, T. Asfour, and R. Dillmann, "Design of the TUAT/Karlsruhe Humanoid Hand," in *IEEE/RSJ International Conference on Intelligent Robots and Systems (IROS)*, Takamatsu, Japan, October 30 - November 5 2000, pp. 1754–1759.
- [22] M. Catalano, G. Grioli, E. Farnioli, A. Serio, C. Piazza, and A. Bicchi, "Adaptive Synergies for the Design and Control of the Pisa/IIT SoftHand," *Int. Journal of Robotics Research*, vol. 33, no. 5, pp. 768–782, 2014.
- [23] A. Bicchi, M. Gabbicini, and M. Santello, "Modelling natural and artificial hands with synergies," *Philosophical Transactions of the Royal Society B: Biological Sciences*, vol. 366, no. 1581, pp. 3153–3161, 2011.
- [24] R. S. Johansson and K. J. Cole, "Grasp stability during manipulative actions," *Canadian journal of physiology and pharmacology*, vol. 72, no. 5, pp. 511–524, 1994.
- [25] M. Gabbicini, A. Bicchi, D. Prattichizzo, and M. Malvezzi, "On the Role of Hand Synergies in the Optimal Choice of Grasping Forces," *Autonomous Robots*, vol. 31, pp. 235–252, 2011.
- [26] R. S. Johansson and J. R. Flanagan, "Coding and use of tactile signals from the fingertips in object manipulation tasks," *Nature Reviews Neuroscience*, vol. 10, pp. 345–359, 2009.
- [27] M. Santello and J. F. Soechting, "Force synergies for multifingered grasping," *Experimental Brain Research*, vol. 133, no. 4, pp. 457–467, 2000.
- [28] M. P. Rearick and M. Santello, "Force synergies for multifingered grasping : effect of predictability in object center of mass and handedness," *Experimental Brain Research*, vol. 144, no. 1, pp. 38–49, 2002.
- [29] J. Starke, K. Chatzilygeroudis, A. Billard, and T. Asfour, "On force synergies in human grasping behavior," in *IEEE/RAS International Conference on Humanoid Robots (Humanoids)*, Toronto, Canada, October 2019, pp. 72–78.
- [30] J. K. Shim and J. Park, "Prehension synergies : principle of superposition and hierarchical organization in circular object prehension," *Experimental Brain Research*, vol. 180, pp. 541–556, 2007.
- [31] R. De Souza, S. El Khoury, J. Santos-Victor, and A. Billard, "Towards comprehensive capture of human grasping and manipulation skills," in *International Symposium on 3D Analysis of Human Movement*, 2014, pp. 84–87.
- [32] R. De Souza, S. El-Khoury, J. Santos-Victor, and A. Billard, "Recognizing the Grasp Intention from Human Demonstration," *Robotics and Autonomous Systems*, vol. 74, pp. 108–121, 2015.
- [33] S. Sundaram, P. Kellnhofer, Y. Li, J.-Y. Zhu, A. Torralba, and W. Matusik, "Learning the signatures of the human grasp using a scalable tactile glove," *Nature*, vol. 569, pp. 698–702, 2019.
- [34] S. Hochreiter and J. Schmidhuber, "Long short-term memory," *Neural Computation*, vol. 9, no. 8, pp. 1735–1780, 1997.
- [35] C. Mandery, O. Terlemez, M. Do, N. Vahrenkamp, and T. Asfour, "The KIT whole-body human motion database," in *International Conference on Advanced Robotics (ICAR)*, Istanbul, Turkey, July 2015, pp. 329–336.
- [36] N. Vahrenkamp, M. Kröhnert, S. Ulbrich, T. Asfour, G. Metta, R. Dillmann, and G. Sandini, "Simox: A robotics toolbox for simulation, motion and grasp planning," in *International Conference on Intelligent Autonomous Systems (IAS)*, 2012, pp. 585–594.
- [37] C. Ferrari and J. Canny, "Planning Optimal Grasps," *1992 IEEE International Conference on Robotics and Automation*, pp. 2290–2295, 1992.
- [38] J. Weisz and P. K. Allen, "Pose Error Robust Grasping from Contact Wrench Space Metrics," *2012 IEEE International Conference on Robotics and Automation*, pp. 557–562, 2012.
- [39] P. Mandikal and K. Grauman, "Learning Dexterous Grasping with Object-Centric Visual Affordances," in *IEEE International Conference on Robotics and Automation*, 2021, pp. 6169–6176.